

ERCOFTAC Series

Martin White · Tala El Samad ·
Ioannis Karathanassis ·
Abdulnaser Sayma · Matteo Pini ·
Alberto Guardone *Editors*

Proceedings of the 4th International Seminar on Non-Ideal Compressible Fluid Dynamics for Propulsion and Power



 Springer

Series Editors

Bernard Geurts, *Faculty of Mathematical Sciences, University of Twente, Enschede, The Netherlands*

Maria Vittoria Salvetti, *Dipartimento di Ingegneria Civile e Industriale, Pisa University, Pisa, Italy*

ERCOFTAC (European Research Community on Flow, Turbulence and Combustion) was founded as an international association with scientific objectives in 1988. ERCOFTAC strongly promotes joint efforts of European research institutes and industries that are active in the field of flow, turbulence and combustion, in order to enhance the exchange of technical and scientific information on fundamental and applied research and design. Each year, ERCOFTAC organizes several meetings in the form of workshops, conferences and summer schools, where ERCOFTAC members and other researchers meet and exchange information. The *ERCOFTAC* series publishes the proceedings of ERCOFTAC meetings, which cover all aspects of fluid mechanics. The series comprises proceedings of conferences and workshops, and of textbooks presenting the material taught at summer schools. The series covers the entire domain of fluid mechanics, which includes physical modelling, computational fluid dynamics including grid generation and turbulence modelling, measuring techniques, flow visualization as applied to industrial flows, aerodynamics, combustion, geophysical and environmental flows, hydraulics, multi-phase flows, non-Newtonian flows, astrophysical flows, laminar, turbulent and transitional flows.

Indexed by SCOPUS, Google Scholar and SpringerLink.

Martin White · Tala El Samad ·
Ioannis Karathanassis · Abdalnaser Sayma ·
Matteo Pini · Alberto Guardone
Editors

Proceedings of the 4th
International Seminar
on Non-Ideal Compressible
Fluid Dynamics for Propulsion
and Power

Editors

Martin White
School of Engineering and Informatics
University of Sussex
Brighton, UK

Tala El Samad
School of Science & Technology
City, University of London
London, UK

Ioannis Karathanassis
School of Science & Technology
City, University of London
London, UK

Abdulnaser Sayma
School of Science & Technology
City, University of London
London, UK

Matteo Pini
Faculty of Aerospace Engineering
Delft University of Technology
Delft, Zuid-Holland, The Netherlands

Alberto Guardone
Department of Aerospace Science
and Technology
Politecnico di Milano
Milan, Italy

ISSN 1382-4309

ISSN 2215-1826 (electronic)

ERCOFTAC Series

ISBN 978-3-031-30935-9

ISBN 978-3-031-30936-6 (eBook)

<https://doi.org/10.1007/978-3-031-30936-6>

© The Editor(s) (if applicable) and The Author(s), under exclusive license to Springer Nature Switzerland AG 2023, corrected publication 2024

This work is subject to copyright. All rights are solely and exclusively licensed by the Publisher, whether the whole or part of the material is concerned, specifically the rights of translation, reprinting, reuse of illustrations, recitation, broadcasting, reproduction on microfilms or in any other physical way, and transmission or information storage and retrieval, electronic adaptation, computer software, or by similar or dissimilar methodology now known or hereafter developed.

The use of general descriptive names, registered names, trademarks, service marks, etc. in this publication does not imply, even in the absence of a specific statement, that such names are exempt from the relevant protective laws and regulations and therefore free for general use.

The publisher, the authors, and the editors are safe to assume that the advice and information in this book are believed to be true and accurate at the date of publication. Neither the publisher nor the authors or the editors give a warranty, expressed or implied, with respect to the material contained herein or for any errors or omissions that may have been made. The publisher remains neutral with regard to jurisdictional claims in published maps and institutional affiliations.

This Springer imprint is published by the registered company Springer Nature Switzerland AG
The registered company address is: Gewerbestrasse 11, 6330 Cham, Switzerland

Preface

The topic of non-ideal compressible fluid dynamics (NICFD) for propulsion and power deals with studying the fluid dynamics of compressible flows for which the ideal gas law does not apply, with an emphasis on reactive and non-reactive flows within power and propulsion systems. The study of NICFD effects finds application within industries that are critical to ensure the provision of clean and secure energy, which includes power generation, refrigeration, heat pumps and clean combustion amongst others.

To understand the field of NICFD, we can break the topic into its constituent parts. The term *non-ideal* relates to the fundamental thermodynamic behaviour of unconventional fluids where the behaviour cannot be predicted assuming the fluid behaves as an ideal gas. Such thermodynamic behaviour can be observed in flows in supercritical states, flows close to the saturation curve, flows close to the critical point and two-phase vapour–liquid flows.

Secondly, we have *compressible fluid dynamics* which relates to the study of fundamental fluid dynamic aspects such as compressible high-speed flows, shockwave formation, boundary layers, turbulence modelling, acoustics and phase change, amongst others. Combining this with non-ideal relates to understanding such fluid behaviour within thermodynamic regions where non-ideal effects are expected. Hand-in-hand with understanding these effects comes the need for computational fluid dynamic, experimental and measurement techniques, developed specifically for such flows.

Finally, *power & propulsion* relates to the application of this knowledge to practical engineering systems operating with non-ideal fluids. This relates to a range of technologies that are becoming, or are likely to become, increasingly important to ensure the provision of clean and secure energy, alongside efficient propulsion. This includes power cycles such as organic Rankine cycles and supercritical carbon dioxide power cycles, refrigeration systems, heat pumps, clean combustion, rocket engines, alongside subsequent system components such as turbomachinery, heat exchangers and combustors.

With this in mind, the seminar themes range from theoretical foundations, to advanced numerical and experimental practices, and to applications. The seminar provides an exciting platform to bring together researchers and scientists who are pioneering theoretical, numerical and experimental advancements in order to share, learn and discuss the latest insights in this field. The key themes of the conference include the following areas: experiments; fundamentals; numerical methods; optimisation and uncertainty quantification; critical and supercritical flows; turbulence and mixing; multi-component fluid flows; applications in ORC power systems; applications in supercritical CO₂ power systems; steam turbines; cryogenic flows; condensing flows in nozzles; cavitating flows and super- and trans-critical fluids in space propulsion.

The biannual NICFD seminar was established in 2016 due to the growing interest in NICFD effects, particularly stemming from advances in propulsion and power applications. The seminar aims to bring together researchers working in the field to discuss

the latest advancements in the field. In 2019, the ERCOFTAC Special Interest Group on Non-Ideal Compressible Fluid Dynamics (SIG-49) was founded (SIG-49), which was setup to further promote the exchange of scientific information and to encourage and consolidate the interaction between NICFD researchers and professionals.

This volume contains the proceedings from NICFD 2022: The 4th International Seminar on Non-Ideal Compressible Fluid Dynamics for Propulsion & Power, which was held during 3–4 November 2022, and hosted by the Thermo-Fluids Research Centre at City, University of London, UK. Further details of the conference can be found here: [NICFD2022](#). The published proceedings are composed of 23 papers reporting on the latest developments in the thematic areas of: Fundamentals; Numerical Modelling and Methods; Multi-phase Flows; Reacting Flows and Experiments.

The conference organisers are extremely grateful to everybody that helped make NICFD 2022 a success. This includes all the authors of the submitted papers, as well as the reviewers and members of the scientific committee, who together ensured a high-quality of the contributions collected here, alongside the accompanying technical presentations. Thanks also go to the City Events team, the session chairs and the student helpers who ensured that the event ran smoothly.

Martin White
Chair

Tala El Samad
Ioannis Karathanassis
Abdulnaser Sayma
Matteo Pini
Conference Co-chairs

Alberto Guardone
Founding Chair

Contents

Fundamentals

Adaptive Simulations of Cylindrical Shock Waves in Polytropic van der Waal Gas	3
<i>Barbara Re, Alessandro Franceschini, and Alberto Guardone</i>	
Non-ideal Compressible Flows in Radial Equilibrium	13
<i>Paolo Gajoni and Alberto Guardone</i>	
Data-Driven Regression of Thermodynamic Models in Entropic Form	22
<i>Matteo Pini, Andrea Giuffrè, Alessandro Cappiello, Matteo Majer, and Evert Bunschoten</i>	

Numerical Modelling and Methods

Direct Numerical Simulation of Wall-Bounded Turbulence at High-Pressure Transcritical Conditions	35
<i>Marc Bernades, Francesco Capuano, and Lluís Jofre</i>	
Development, Validation and Application of an ANN-Based Large Eddy Simulation Subgrid-Scale Turbulence Model for Dense Gas Flows	43
<i>Alexis Giauque, Aurélien Vadrot, and Christophe Corre</i>	
Bypass Laminar-Turbulent Transition on a Flat Plate of Organic Fluids Using DNS Method	53
<i>Bijie Yang, Tao Chen, and Ricardo Martinez-Botas</i>	
High Fidelity Simulations and Modelling of Dissipation in Boundary Layers of Non-ideal Fluid Flows	62
<i>Francesco Tosto, Andrew Wheeler, and Matteo Pini</i>	
Estimating Model-Form Uncertainty in RANS Turbulence Closures for NICFD Applications	72
<i>Giulio Gori</i>	
Assessment of Density and Compressibility Corrections for RANS Simulations of Real Gas Flows Using SU2	82
<i>D. Schuster, Y. Ince, Alexis Giauque, and Christophe Corre</i>	

Validation of the SU2 Fluid Dynamic Solver for Isentropic Non-Ideal Compressible Flows	91
<i>Blanca Fuentes-Monjas, Adam J. Head, Carlo De Servi, and Matteo Pini</i>	

Multi-phase Flows

Numerical Validation of a Two-Phase Nozzle Design Tool Based on the Two-Fluid Model Applied to Wet-to-Dry Expansion of Organic Fluids	103
<i>Pawel Ogrodniczak and Martin T. White</i>	

Numerical Modelling of Cryogenic Flows Under Near-Vacuum Pressure Conditions	114
<i>Theodoros Lyras, Ioannis K. Karathanassis, Nikolaos Kyriazis, Phoivos Koukouvinis, and Manolis Gavaises</i>	

About the Effect of Two-Phase Flow Formulations on Shock Waves in Flash Metastable Expansions Simulations	125
<i>Egoi Ortego Sampedro</i>	

Non-equilibrium Phenomena in Two-Phase Flashing Flows of Organic Fluids	135
<i>Carlotta Tammone, Alessandro Romei, Giacomo Persico, and Fredrik Haglind</i>	

A Pressure-Based Model for Two-Phase Flows Under Generic Equations of State	146
<i>Barbara Re, Giuseppe Sirianni, and Rémi Abgrall</i>	

Validation and Application of HEM for Non-ideal Compressible Fluid Dynamic	156
<i>Liyi Chen, Michael Deligant, Mathieu Specklin, and Sofiane Khelladi</i>	

Reacting Flows

Numerical Simulations of Real-Fluid Reacting Sprays at Transcritical Pressures Using Multiphase Thermodynamics	169
<i>Mohamad Fathi, Stefan Hickel, and Dirk Roekaerts</i>	

Experiments

Grid-Generated Decaying Turbulence in an Organic Vapour Flow	181
<i>Leander Hake, Stefan aus der Wiesche, Stephan Sundermeier, Aurélien Bienner, Xavier Gloerfelt, and Paola Cinnella</i>	

Study on the Operation of the LUTsCO ₂ Test Loop with Pure CO ₂ and CO ₂ + SO ₂ Mixture Through Dynamic Modeling	191
<i>Giuseppe Petrucci, Teemu Turunen-Saaresti, Aki Grönman, and Afonso Lugo</i>	
Preliminary Experiments in High Temperature Vapours of Organic Fluids in the Asymmetric Shock Tube for Experiments on Rarefaction Waves (ASTER)	201
<i>Nitish Chandrasekaran, Theodoros Michelis, Bertrand Mercier, and Piero Colonna</i>	
Experimental and Numerical Study of Transonic Flow of an Organic Vapor Past a Circular Cylinder	209
<i>Stephan Sundermeier, Camille Matar, Paola Cinnella, Stefan aus der Wiesche, Leander Hake, and Xavier Gloerfelt</i>	
Loss Measurement Strategy in ORC Supersonic Blade Cascades	217
<i>Marco Manfredi, Giacomo Persico, Andrea Spinelli, Paolo Gaetani, and Vincenzo Dossena</i>	
Mach Number Estimation and Pressure Profile Measurements of Expanding Dense Organic Vapors	229
<i>Adam J. Head, Theodoros Michelis, Fabio Beltrame, Blanca Fuentes-Monjas, Emiliano Casati, Carlo De Servi, and Piero Colonna</i>	
Correction to: Proceedings of the 4th International Seminar on Non-Ideal Compressible Fluid Dynamics for Propulsion and Power	C1
<i>Martin White, Tala El Samad, Ioannis Karathanassis, Abdulnaser Sayma, Matteo Pini, and Alberto Guardone</i>	
Author Index	239

Fundamentals



Adaptive Simulations of Cylindrical Shock Waves in Polytrropic van der Waal Gas

Barbara Re^(✉), Alessandro Franceschini, and Alberto Guardone

Department of Aerospace Science and Technology, Politecnico di Milano,
Milano, Italy

{barbara.re,alberto.guardone}@polimi.it,
alessandro1.franceschini@mail.polimi.it

Abstract. The propagation of converging cylindrical shock waves, collapsing at the axis of symmetry, in a non-ideal gas is investigated by using innovative interpolation-free mesh adaptation techniques. The high pressure, temperature, and energy that can be reached close to the focus point call for thermodynamic models able to take into account the non-ideal gas effects. A distinguishing feature of converging shock waves is the non-constant propagation speed, which makes the flow field behind the shock intrinsically unsteady. To efficiently simulate this configuration, it is fundamental to adapt the computational domain as time evolves. Hence, at each time step, we modify the grid spacing through node insertion, deletion, or relocation according to the current position of the flow features. In this work, any interpolation of the solution between the original and the adapted grids is avoided thanks to a peculiar strategy able to describe mesh adaptation within the arbitrary Lagrangian-Eulerian framework. The adaptive simulation framework, equipped with the polytrropic van der Waals equation of state, is assessed first in dilute conditions, where it is possible to compare numerical results with theoretical predictions. In particular, we compute the Guderley-like self-similar solution describing shocks of different intensities propagating in the siloxane MM. Then, it is used to verify the possibility to reach higher energy density when the shock is initiated in the NICFD regime. Finally, we investigate the interaction between the converging shock wave and an arc-shaped obstacle, which is a fundamental phase of the so-called reshaping process, useful to increase the stability of converging shocks.

Keywords: cylindrical shock waves · van der Waals model · mesh adaptation · finite volume scheme

1 Introduction

Converging cylindrical shock waves, collapsing at the axis of symmetry, have been investigated in several theoretical, numerical, and experimental campaigns since the first half of last century [5, 7]. Differently from the planar case, converging shocks are intrinsically unsteady phenomena, because the speed of the

shock increases as the radius decreases. Hence, during the propagation towards the focus point, the shock intensity increases, reaching particularly high values of fluid temperature and pressure close to the focus point. The possibility to reach such a high-energy condition has prompted many research activities, motivated by the potential applications in different fields, spanning from medical treatments, e.g., lithotripsy for renal calculi, to power generation, for instance, for the ignition of the nuclear fusion process [1]. Unfortunately, the stability of these flow structures, defined as the capability of the converging wave to approach the cylindrical shape damping out disturbances during the propagation, is of great concern, because small perturbations can make the propagation front deviate from the cylindrical shape [7]. The stability decreases also as the shock Mach number increases. A possible strategy to prevent the onset of instabilities is the so-called *shock-reshaping* process, which turns a cylindrical shock into a prismatic one through controlled reflections. To minimize the possible losses that would reduce the shock intensity, these reflections are generated by lenticular obstacles, i.e., symmetric aerodynamic profiles with sharp leading and trailing edge [6].

The aim of this work is the assessment of a numerical simulation tool for 2D cylindrical converging shocks, without and with obstacles, in non-ideal compressible fluid dynamic regimes, where, for the same pressure jump, higher temperature and energy are reached. The proposed CFD tool performs unsteady inviscid flow simulations using a mesh adaptation strategy, which refines and makes the grid coarser following the shock evolution. Notably, this adaptation is performed within the arbitrary Lagrangian-Eulerian (ALE) framework, so that no interpolation of the solution from the original to the adapted grid is required [2, 8]. The siloxane MM is the chosen working fluid for the tests here presented and its thermodynamic behavior is described by the polytropic van der Waals model.

This work represents the first step of a wider project, whose long-term goal is the study of how the obstacle geometry and the fluid dynamic behavior affect the intensity and the stability of the converging shock waves.

2 The Numerical Method

Assuming the flow as inviscid, i.e., neglecting thermal conductivity and viscosity, the fluid flow behavior is described by the unsteady compressible Euler equations. To close the system, the van der Waals equation of state (EOS) is considered:

$$p = \frac{RT}{v-b} - \frac{a}{v^2} \quad (1)$$

where p is the pressure, T the temperature, v the specific volume, R the gas constant, and a and b are the fluid-specific parameters of the van der Waals equation that account for non-ideal gas effects about covolume and intermolecular attractive forces. To a first approximation and to compare numerical results with theoretical predictions, the polytropic assumption is made. So, the value of

the specific heat at constant volume c_v is computed through the Aly-Lee equation [3] at $T = 300$ K, and it is assumed to be constant during the simulation, even though the high temperatures and the low densities that can be reached at the focus point could jeopardize the hypothesis of polytropic gas [12].

2.1 The Unsteady Adaptive Finite Volume Scheme

The governing equations are integrated in space over an unstructured, triangular mesh that discretizes the domain Ω , through a node-centered, edge-based finite volume scheme. The equations are discretized within an ALE framework that allows the finite volumes to move and deform independently from the flow velocity. Thanks to a peculiar three-step procedure, also the topology changes due to mesh adaptation—such as node insertion, node deletion, and edge swapping—are described within a standard ALE formulation [8]. A backward-finite-difference implicit scheme with a dual time-step technique is used as time integrator.

The unsteady adaptive discretization strategy is well-suited for the simulation of the converging shock waves because the mesh can be modified to follow moving flow features: as shown in Fig. 1, the minimum grid spacing is reached only close to the shock wave, increasing the accuracy while keeping the number of grid nodes under control. The adaptation process is driven by criteria based on the derivatives of the flow variables: where large variations are detected, the local grid spacing is reduced, whereas it is enlarged where the solution is smooth, without jeopardizing solution accuracy [9, 10]. The adaptation criterion is a weighted combination of the magnitude of the Hessian of the Mach number and the gradient of the density, with weights 0.8 and 0.2, respectively. The same strategy can be used also to follow arbitrarily large displacements of the boundary domain [11], but in this work we consider only a domain with fixed boundaries.

Due to the axial symmetry of the numerical domain, the computational cost is reduced by considering only a slice of the 2D cylinder section. The computational domain, shown in Fig. 1, is thus defined by three boundaries: the lower and the upper walls that merge at the focus point, which are modeled as inviscid walls, and the external boundary shaped as an arc of a circle, where non-reflecting boundary conditions are imposed.

The simulations are initialized with null velocity, and a jump in pressure and density at a certain radial distance (R_0) from the focus point, hence with a radial version of the Riemann problem. The post-shock density is computed according to the Rankine-Hugoniot adiabatic jump relations for a perfect gas, as in [13]. After the diaphragm rupture, a shock wave and a contact discontinuity propagate inward, while a rarefaction fan propagates outward. We remind that, unlike the planar case, the internal, i.e., post-shock, state is time-dependent because the shock intensity increases while converging.

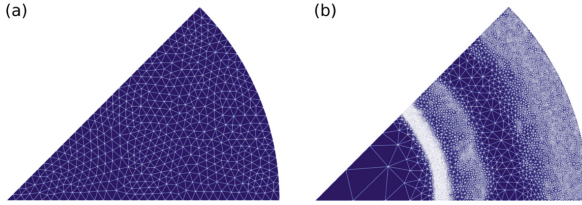


Fig. 1. Computational domain: a) initial grid, with a uniform grid spacing $h_0 = 0.01$ m; b) example of an adapted grid obtained during the simulation. The radial length of the mesh is 0.31 m. During adaptation, the imposed minimum edge size is $h_{\min} = 0.001$ m

2.2 Characterization of Converging Shock Waves

The evolution of cylindrical shock waves can be approximated according to Guderley's law [5]:

$$\frac{R_s}{R_0} = \left(1 - \frac{t}{\tilde{\tau}}\right)^\alpha, \quad (2)$$

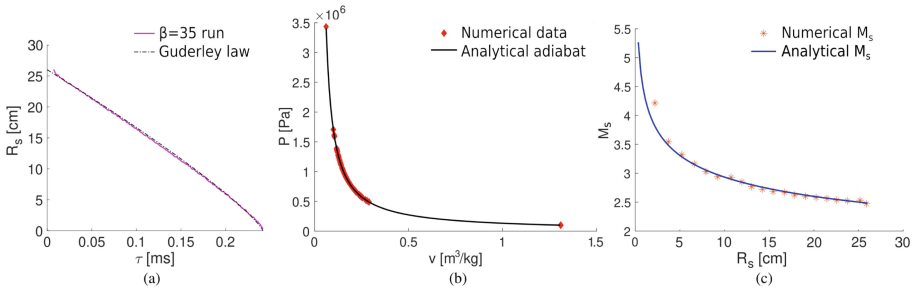


Fig. 2. Comparison of numerical data and theoretical predictions for the MM in dilute conditions, for the $\beta = 35$ case.

which expresses the shock position R_s as function of the time t . R_0 is the initial shock radius and $\tilde{\tau}$ the total focusing time, namely the time required by the shock to reach the focus point. Finally, α is the self-similarity exponent, which is a function of shock geometry (planar, cylindrical, or spherical) and thermodynamics of the gas. For the ideal gas, the theoretical value of α for cylindrical shocks is 0.834, while in this work, the numerical value according to the van der Waals EOS is computed through a non-linear least squares approach with numerical data.

A further theoretical result useful for validation is the post-shock pressure along the Hugoniot adiabetic curve, according to the van der Waals model, which can be defined in the p - v plane as

$$p_2 = p_2(p_1, v_1, v_2) = \left[\frac{1}{\delta_\gamma} \left(p_1 + \frac{a}{v_1^2} \right) (v_2 - b) - \frac{1}{2} p_1 (v_2 - v_1) + \frac{a}{v_2 \delta_\gamma} \left(\frac{b}{v_2} - 1 \right) \right] / \left[\left(\frac{1}{2} + \frac{1}{\delta_\gamma} \right) v_2 - \left(\frac{v_1}{2} + \frac{b}{\delta_\gamma} \right) \right], \quad (3)$$

where $\delta_\gamma = R/c_v$, and the subscripts 1 and 2 refer to the pre- and post-shock state, respectively.

Finally, the monotonic behavior of the shock front intensity is evaluated by computing the shock Mach number as a function of the shock radius. To do so, Guderley's law is derived with respect to time as:

$$M_S^G(t_k) = \frac{1}{c_1} \cdot \left| \frac{\partial R_s(t_k)}{\partial t} \right|_{t_k} = \frac{R_s \cdot \alpha}{c_1 \cdot (\bar{\tau} - t_k)}, \quad (4)$$

where c_1 is the pre-shock speed of sound and t_k is the k -th time step.

From the numerical results, we compute the shock position R_s in the radial direction in a post-process step by using an ad-hoc algorithm, devised following the three criteria proposed by Vignati and Guardone [13]. We evaluate the post-shock state through a similar strategy, but, due to the fact the shock wave is represented over more than one cell due to numerical viscosity, it is extracted at a position $R_e \geq R_s$, and R_e is computed by solving a local maximum problem of the second order derivative of the pressure in the proximity of R_s [4].

3 Results

Simulations of converging shock waves with siloxane MM are now presented. Different values of the pressure jump $\beta = p_2/p_1$ across the diaphragm of the numerical Riemann problem are tested. In the first case, we consider $\beta = 35$, with $p_1 = 0.0516 p_c$ and density $\rho_1 = 0.0039 \rho_c$, namely in dilute gas conditions (the subscript c indicates critical variables), where a fair agreement with the perfect gas model is expected. The diaphragm is located at $R_0 = 26$ cm, whereas the domain length in the radial direction is 31 cm. The numerical results and the theoretical predictions are compared in Fig. 2. The shock position, in panel (a), is compared with the theoretical Guderley's law with the ideal gas self-similar exponent $\alpha = 0.834$. The fitted value of α results equal to 0.852, deviating about 2% from the ideal gas model case, in these dilute conditions. In Fig. 2(b), post-shock states computed from the numerical simulation are plotted along with the shock adiabetic curve in the p - v plane, observing a good agreement. Starting from the pivot state, namely the one at the highest specific volume, throughout its propagation, the converging shock wave progressively increases the fluid post-shock pressure, eventually attaining values in the order of GPa. The latest comparison for this validation case is the shock Mach number as a

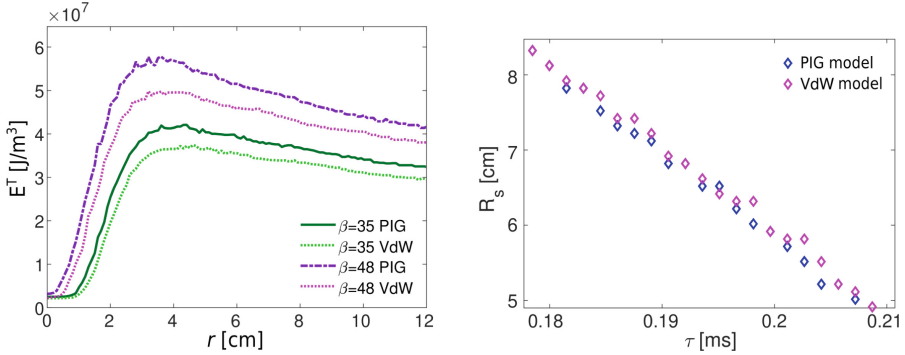


Fig. 3. Comparison between the results for the MM siloxane in dilute conditions, modelled with ideal and van der Waals EOS. Left: total energy close to the focus point; right: shock position close to focus point.

function of shock radius, through Eq. (4), where, again, a good agreement is achieved and the Mach number of the shock front monotonically increases as the shock propagates. More specifically, from Fig. 2(c), it can be seen that the region close to the focus point is characterized by a higher slope of the curve, meaning that the last instants of the convergence process are contributing the most to the increase of fluid energy. This is the reason behind the importance of keeping as stable as possible the shock front during the implosion process in practical applications.

Now, the importance and influence of the selected thermal EOS to model the fluid behavior are assessed, considering the same numerical setup for each test. Tested values of pressure jump are $\beta = 35$ and $\beta = 48$. Relevant fluid dynamics variables are sampled from probes located along a radial coordinate r . Figure 3 (left) shows the differences in the total energy density, at two different time instants, one for each value of β . The differences in energy are important, especially once the converging shock has reached the focus point. Pressure values are lower with van der Waal EOS than with the perfect gas because attractive forces reduce fluid pressure at a given thermodynamic state. Consequently, lower pressure means lower temperature and lower total energy E^T . Moreover, results with the van der Waals model are characterized by larger values of shock radius at a given time, which reflect eventually into Guderley's law. Indeed, looking at the region close to the focus point, reported in Fig. 3 (right), the ideal gas confirms its tendency of overestimating the shock wave speed to the van der Waals model, because, at a given time step, lower values of shock radius are determined by a higher shock wave speed.

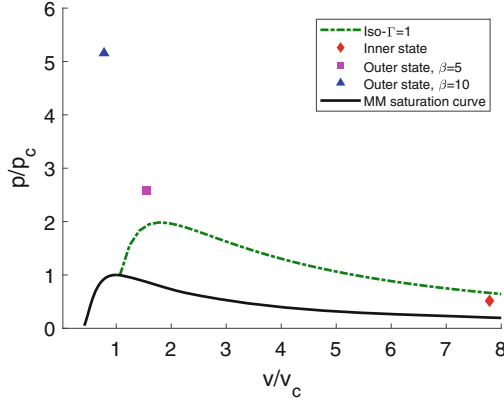


Fig. 4. Initial Riemann problem states for the tests with siloxane MM in NICFD conditions. The saturation curve is drawn in black, along with the isoline at $\Gamma = 1$ that delimits the NICFD region. The red marker denotes the initial, pre-shock, state. The blue and the violet markers depict, respectively, the post-shock state corresponding to $\beta = 5$, and $\beta = 10$, respectively.

Converging shock waves are then simulated in the non-ideal regime, which is bounded by $\Gamma = 1$ iso-line and is characterized by classical gas dynamics features, but the speed of sound dependence on the density is the opposite to the ideal regime. The initial conditions, displayed in Fig. 4, are $p_1 = 0.5157 p_c$ and $\rho_1 = 0.1284 \rho_c$, and two values of pressure jumps are simulated, $\beta = 5$ and $\beta = 10$. Shock position in time is depicted in Fig. 5 and it qualitatively agrees with the behavior predicted by Guderley's law. Moreover, the extrapolated power law exponents α computed for the two different β values show a variation lower than 1%, as proof of the validity of the implemented framework.

To evaluate if the compression factor attained in the proximity of the focus point is enhanced due to initial dense working conditions, the behavior of the pressure coefficient trace, defined as $c_p = \frac{p}{p_1}$, is investigated by computing the trace at the first probe (located at $r = 0.001$ m), shown in Fig. 6. As expected, starting from the same pre-shock conditions, higher values of β are associated with lower total focusing time, since the shock wave converges faster. In fact, the trace peak for $\beta = 10$ is reached at an earlier time. Moreover, doubling the pressure jump β , the maximum pressure coefficient value increases from $c_p^{\max} = 42.4$ to $c_p^{\max} = 106.4$, so it increases more than twice. This super-linear proportionality of the pressure coefficient on the pressure jump has been observed only in the non-ideal regime. Hence, working in dense conditions, with an initial condition close to the saturation curve, could lead easier to higher gas energy states at the focus point, which is an aspect of primary importance for practical applications of cylindrical converging shock waves.

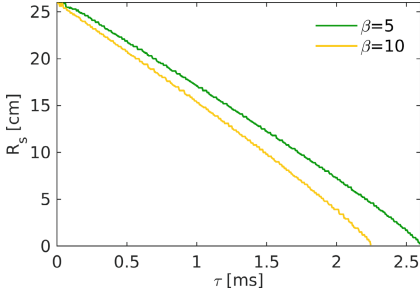


Fig. 5. Guderley’s law from numerical simulation of MM siloxane in NICFD conditions.

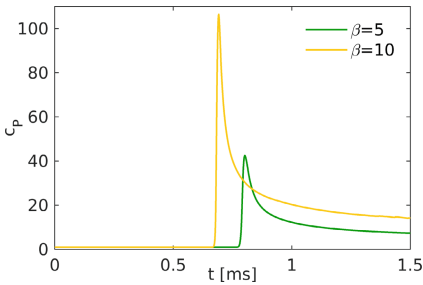


Fig. 6. Pressure coefficient traces in NICFD conditions at $r = 0.001$ m.

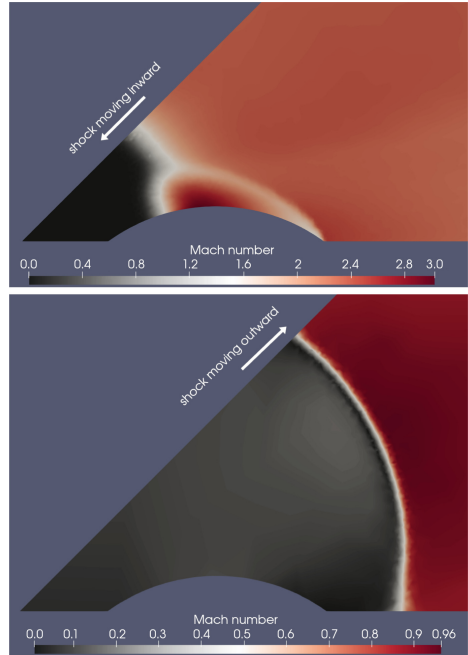


Fig. 7. Mach number contour plots for the test with the obstacle, in dense condition, at a time instant before (top) and after (bottom) the focus time.

Finally, a numerical simulation of a cylindrical converging shock wave that interacts with an obstacle is performed. The obstacle is an arc-shaped profile located in the proximity of the focus point, which generates a truly 2D flow field. Figure 7 (left) shows the Mach reflection caused by the shock-obstacle interaction. This flow structure, composed by the incident shock, the reflected shock and the third shock that travels parallel to the surface called Mach stem, is required to obtain cylindrical shock reshaping, regardless of the reflection type occurring in correspondence with the obstacle leading edge [13]. The robustness of the developed framework for adaptive 2D simulations of cylindrical shock waves has been proven through the computation of the flow field behavior also after the focus point is reached. Figure 7 (right) shows the Mach field when the shock wave has already been reflected at the focus point and passed the obstacle.

4 Conclusions

For the first time, 2D interpolation-free adaptive simulations of cylindrical converging shock waves have been carried out, assessing the validity of an innovative unsteady solver for the ALE formulation of the Euler equations over adaptive

grids in NICFD regimes. The siloxane MM has been modeled through the van der Waals EOS, accounting for non-ideal gas effects. Several initial jump conditions for the radial Riemann problem have been tested, along with the effects of the thermodynamic model. The ideal gas model proved to overestimate the propagation velocity of the converging shock, even in dilute conditions. The simulations in the NICFD regime demonstrated that working in such conditions is efficient to obtain a higher energy state of the gas in close proximity to the focus point. Finally, the ultimate purpose of this work has been about the numerical simulation of a converging shock wave that eventually interacts with an obstacle, undergoing a reshaping process. In practical applications, reshaping into polygonal shocks is exploited since the latter are more stable. Results showed how the numerical method adopted is suitable for this type of problem. The Mach reflection pattern leading to the shock wave reshaping has been simulated. Moreover, the robustness of the method permits to represent properly the flow field once the converging shock wave has reached the focus point and is bounced back, moving outwards the computational domain.

References

1. Clark, D., Tabak, M.: A self-similar isochoric implosion for fast ignition. *Nucl. Fusion* **47**, 1147–1156 (2007). <https://doi.org/10.1088/0029-5515/47/9/011>
2. Colombo, S., Re, B.: An ALE residual distribution scheme for the unsteady Euler equations over triangular grids with local mesh adaptation. *Comput. Fluids* **239**, 105414 (2022). <https://doi.org/10.1016/j.compfluid.2022.105414>
3. Colonna, P., Nannan, N.R., Guardone, A., Lemmon, E.W.: Multiparameter equations of state for selected siloxanes. *Fluid Phase Equilib.* **244**, 193–211 (2006). <https://doi.org/10.1016/j.fluid.2006.04.015>
4. Franceschini, A.: Cylindrical shock waves in high molecular complexity van der Waals fluid. Master’s thesis, Politecnico di Milano, July 2022
5. Guderley, K.G.: Stark kugelige und zylindrische verdichtungsstöße in der nähe des kugelmittelpunktes bzw. der zylinderachse. *Luftfahrtforschung* **19**, 302 (1942)
6. Kjellander, M., Tillmark, N., Apazidis, N.: Thermal radiation from a converging shock implosion. *Phys. Fluids* **22**(4), 046102 (2010). <https://doi.org/10.1063/1.3392769>
7. Perry, R.W., Kantrowitz, A.: The production and stability of converging shock waves. *J. Appl. Phys.* **22**, 878–886 (1951). <https://doi.org/10.1063/1.1700067>
8. Re, B., Dobrzynski, C., Guardone, A.: An interpolation-free ALE scheme for unsteady inviscid flows computations with large boundary displacements over three-dimensional adaptive grids. *J. Comput. Phys.* **340**, 26–54 (2017). <https://doi.org/10.1016/j.jcp.2017.03.034>
9. Re, B., Dobrzynski, C., Guardone, A.: Assessment of grid adaptation criteria for steady, two-dimensional, inviscid flows in non-ideal compressible fluids. *Appl. Math. Comput.* **319**, 337–354 (2018). <https://doi.org/10.1016/j.amc.2017.03.049>
10. Re, B., Guardone, A.: An adaptive ALE scheme for non-ideal compressible fluid dynamics over dynamic unstructured meshes. *Shock Waves* **29**, 73–99 (2019). <https://doi.org/10.1007/s00193-018-0840-2>

11. Re, B., Guardone, A., Dobrzynski, C.: An adaptive conservative ALE approach to deal with large boundary displacements in three-dimensional inviscid simulations. In: 55th AIAA Aerospace Sciences Meeting, Grapevine, Texas, 9–13 January 2017 (2017). <https://doi.org/10.2514/6.2017-1945>
12. Vignati, F.: Dynamics of cylindrical converging shock waves interacting with circular-arc obstacles. Ph.D. thesis, Politecnico di Milano (2015)
13. Vignati, F., Guardone, A.: Dynamics of cylindrical converging shock waves interacting with aerodynamic obstacle arrays. *Phys. Fluids* **27**, 066101 (2015). <https://doi.org/10.1063/1.4921680>



Non-ideal Compressible Flows in Radial Equilibrium

Paolo Gajoni and Alberto Guardone^(✉)

Politecnico di Milano, Milan, Italy
{paolo.gajoni, alberto.guardone}@polimi.it

Abstract. Compressible flows at radial equilibrium, *i.e.* θ -independent flows, are investigated in the ideal, dilute-gas regime and in the non-ideal regime close to the liquid-vapour saturation curve and the critical point. A differential relation for the Mach number dependency on the radius is derived for both ideal and non-ideal conditions. For ideal flows, the relation is integrated analytically.

For flows of low molecular complexity fluids, such as diatomic nitrogen or carbon dioxide, the Mach number is a monotonically decreasing function of the radius of curvature, with the polytropic exponent γ being the only fluid-dependent parameter. In non-ideal conditions, the Mach number profile depends also on the total thermodynamic conditions of the fluid. For high molecular complexity fluids, such as toluene and MM (hexamethyldisiloxane), a non-monotone Mach profile is uncovered for non-ideal flows in supersonic conditions. For Bethe-Zel'dovich-Thompson fluids, the non-monotone behaviour is possible also in subsonic conditions.

Keywords: Non-ideal Compressible Fluid Dynamics (NICFD) · non-ideal flows · radial equilibrium

1 Introduction

Flows of molecularly complex fluids in the neighbourhood of the liquid-vapour saturation curve and the critical point significantly depart from the ideal-gas behaviour typical of dilute thermodynamic states. Thompson [14] firstly noted the crucial role of the so-called fundamental derivative of gas dynamics,

$$\Gamma = \frac{v^3}{2c^2} \left(\frac{\partial^2 P}{\partial v^2} \right)_s = 1 + \frac{c}{v} \left(\frac{\partial c}{\partial P} \right)_s, \quad (1)$$

in outlining the dynamic behaviour of compressible flows in non-ideal conditions. Different gasdynamic regimes can be defined, based on the value of Γ . Flows developing through thermodynamic states featuring $\Gamma > 1$ are said to evolve in the ideal gasdynamic regime, since the usual behaviour of ideal gases is observed. By contrast, one speaks of non-ideal regime, if the flow evolution possibly experiences values of $\Gamma < 1$, or non-classical regime, when negative values of Γ are reached. The most unconventional phenomena include, for $\Gamma < 1$, the Mach number decrease in steady supersonic

nozzles and around rarefactive ramps [4,5,8,13] and the increase of the Mach number across oblique shock waves [16], whereas expansion shock waves and split waves are characteristic of the non-classical regime [12,15]. State-of-the-art thermodynamic models [3,10] predict values of $\Gamma < 1$ in the vapour-phase region close to saturation for fluids with high molecular complexity [1], or even $\Gamma < 0$ for the so-called Bethe-Zel'dovich-Thompson (BZT) fluids. Unfortunately, no experimental evidence of the occurrence of $\Gamma < 0$ is available, yet [7,11].

2 Scope of Research

Two-dimensional compressible flows at radial equilibrium, *i.e.* θ -independent flows, assuming a polar representation of the flowfield shown in Fig. 1, are here investigated. Formally, they represent the flow within an annulus, in which the curvature is constant with θ , but they can also be illustrative of the behaviour of flows subjected to a strong curvature. The subject of this paper is in fact inspired by the behaviour of a flow within a turbine cascade, which is repeatedly deviated through alternating rotors and stators. The curvature prescribed by the passage between two adjacent blades of an Organic Rankine Cycle (ORC) turbine disk [2], for example, can be seen in Fig. 2.

The research, however, does not deal directly with turbomachine flows, but it just aims at describing simple two-dimensional flows, which are mainly of theoretical interest. The purpose is in fact to derive a differential relation for the Mach number dependency on the radius of curvature, for flows at equilibrium, in both ideal and non-ideal conditions. For ideal flows, the relation, henceforth called radial equilibrium equation, is integrated analytically.

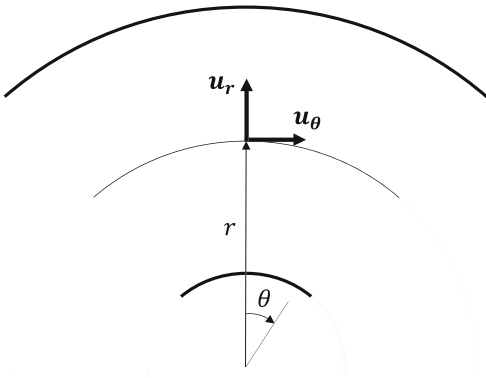


Fig. 1. Radial equilibrium flow representation.



Fig. 2. Example of an ORC turbine disk [9].

3 Compressible Flows at Radial Equilibrium

In an attempt to obtain a simple, and possibly closed-form, solution, several simplifying hypotheses are taken into account. A steady flow of a single-phase monocomponent fluid is investigated, under the assumptions of null heat transfer and viscous effects. The flow is therefore homototalenthalpic ($h_t = \text{const.} = \bar{h}_t$) and homoentropic ($s = \text{const.} = \bar{s}$).

The compressible Euler equations in polar coordinates are taken as starting point for the derivation of the radial equilibrium equation. Exploiting the above hypotheses, the continuity and momentum equations lead to the intuitive definition of the pressure gradient established due to the curvature,

$$\frac{dP}{dr} = \rho \frac{u_\theta^2}{r} = \rho \frac{u^2}{r} \quad (2)$$

where r represents the radial coordinate and $u_\theta = u$ is the flow velocity, pointing in the θ -direction, already shown in Fig. 1. Through the definitions of the speed of sound c and the Mach number $M = u/c$, an equivalent expression for the density gradient can be obtained:

$$\frac{d\rho}{dr} = \left(\frac{\partial \rho}{\partial P} \right)_s \frac{dP}{dr} = \frac{1}{c^2} \frac{dP}{dr} = \rho \frac{M^2}{r}. \quad (3)$$

The specification of a thermodynamic model finally yields the expression for the Mach variation along the radius. The most general formulation is achieved exploiting sophisticated models able to describe gases behaviour even in non-ideal conditions. In this context, a non-dimensional measure of the Mach derivative with the density is introduced [4] as

$$J = \frac{\rho}{M} \frac{dM}{d\rho} = 1 - \Gamma - \frac{1}{M^2}. \quad (4)$$

The Mach number variation with the radius is therefore computed:

$$\frac{dM}{dr} = \frac{dM}{d\rho} \frac{d\rho}{dr} = \frac{M}{\rho} \left(1 - \Gamma - \frac{1}{M^2} \right) \rho \frac{M^2}{r} = \frac{M}{r} [(1 - \Gamma)M^2 - 1]. \quad (5)$$

The above equation is then recast in non-dimensional form by defining a dimensionless radial coordinate $\tilde{r} = r/r_i$, where r_i represents the internal radius of the channel where the radial equilibrium is established.

The final expression reads

$$\frac{dM}{d\tilde{r}} = -\frac{M}{\tilde{r}} [1 + (\Gamma - 1)M^2]. \quad (6)$$

The possibility to write the radial equilibrium equation as a function of \tilde{r} proves that the same solution is valid for all possible values of the internal radius of curvature and the only parameter that matters is the width of the curve, *i.e.* the external radius r_e . Equation (6) can eventually be modified exploiting Eq. (4), yielding

$$\frac{dM}{d\tilde{r}} = \frac{M^3}{\tilde{r}} J. \quad (7)$$